

1 **Disruption of glucagon receptor signaling causes hyperaminoacidemia exposing a possible**
2 **liver - alpha-cell axis**

3 Katrine D. Galsgaard^{1,2}, Marie Winther-Sørensen^{1,2}, Cathrine Ørskov¹, Hannelouise Kissow^{1,2},
4 Steen S. Poulsen¹, Hendrik Vilstrup³, Cornelia Prehn⁴, Jerzy Adamski^{4,5,6}, Sara L. Jepsen^{1,2}, Bolette
5 Hartmann^{1,2}, Jenna Hunt^{1,2}, Maureen J. Charron⁷, Jens Pedersen^{1,2}, Nicolai J. Wewer Albrechtsen^{1,2},
6 Jens J. Holst^{1,2}.

7 *1: Department of Biomedical Sciences, Faculty of Health and Medical Sciences, University of*
8 *Copenhagen, Copenhagen, Denmark*

9 *2: Novo Nordisk Foundation Center for Basic Metabolic Research, Faculty of Health and Medical*
10 *Sciences, University of Copenhagen, Copenhagen, Denmark*

11 *3: Department of Hepato-Gastroenterology, Aarhus University hospital, Aarhus, Denmark*

12 *4: Institute of Experimental Genetics, Genome Analysis Center, Helmholtz Zentrum, German*
13 *Research Center for Environmental Health, Ingolsädter Landße 1, München-Nueherberg, Germany*

14 *5: Lehrstul für Experimentelle Genetik, Technishe Universität München, Freising-Weihestephan,*
15 *Germany*

16 *6: German Center for Diabetes Research (DZD), München-Nueherberg, Germany*

17 *7: Departments of Biochemistry, Obstetrics and Gynecology and Women's Health, and Medicine,*
18 *Albert Einstein College of Medicine, New York, USA*

19

20 **Running head:** Disruption of glucagon signaling causes hyperaminoacidemia

Disruption of glucagon signaling causes hyperaminoacidemia

21 **Correspondence:** Professor Jens J. Holst, Department of Biomedical Sciences, Faculty of Health
22 and Medical Sciences, University of Copenhagen, Blegdamsvej 3B, 2200 Copenhagen, Denmark;
23 Telephone +45 35327518; E-mail: jjholst@sund.ku.dk

24

25 **Abstract**

26 Glucagon secreted from the pancreatic alpha-cells is essential for regulation of blood glucose levels.
27 However, glucagon may play an equally important role in the regulation of amino acid metabolism
28 by promoting ureagenesis. We hypothesized that disruption of glucagon receptor signaling would
29 lead to an increased plasma concentration of amino acids, which in a feedback manner stimulates
30 the secretion of glucagon, eventually associated with compensatory proliferation of the pancreatic
31 alpha-cells.

32 To address this, we performed plasma profiling of glucagon receptor knockout (*Gcgr*^{-/-}) mice and
33 wild-type (WT) littermates using liquid chromatography mass spectrometry (LC-MS)-based
34 metabolomics, and tissue biopsies from the pancreas were analyzed for islet hormones and by
35 histology. A principal component analysis of the plasma metabolome from *Gcgr*^{-/-} and WT
36 littermates indicated amino acids as the primary metabolic component distinguishing the two groups
37 of mice. Apart from their hyperaminoacidemia, *Gcgr*^{-/-} mice display hyperglucagonemia, increased
38 pancreatic content of glucagon and somatostatin (but not insulin), and alpha-cell hyperplasia and
39 hypertrophy compared to WT littermates. Incubating cultured α -TC1.9 cells with a mixture of
40 amino acids (Vamin 1%) for 30 minutes and for up to 48 hours led to increased glucagon
41 concentrations (~six-fold) in the media and cell proliferation (~two-fold), respectively. In
42 anesthetized mice, a glucagon receptor specific antagonist (Novo Nordisk 25-2648, 100 mg/kg)
43 reduced amino acid clearance. Our data supports the notion that glucagon secretion and hepatic
44 amino acid metabolism are linked in a close feedback loop, which operates independently of normal
45 variations in glucose metabolism.

46 **Keywords:** Alpha-cell, Amino Acids, Glucagon, Glucagon Receptor, Hyperglucagonemia.

47 **Introduction**

48 Glucagon is a peptide-hormone of 29 amino acids processed from the prohormone, proglucagon, by
49 pro-hormone convertase 2 (PC-2) in pancreatic alpha-cells (39). Activation of the hepatic glucagon
50 receptor (GR) increases hepatic glycogenolysis and gluconeogenesis (10), and the physiological
51 role of glucagon has been coupled to glucose metabolism with opposing actions to insulin (1, 28,
52 43). However, several studies have suggested that glucagon may play an equally important role in
53 the regulation of hepatic amino acid metabolism (2, 5, 7, 13, 21, 41). Increased fasting and
54 postprandial plasma concentrations of glucagon have been reported in clinical conditions including
55 non-alcoholic fatty liver disease (NAFLD) and type 2 diabetes (33) raising the question whether this
56 is related to amino acid metabolism.

57 Knockout of the GR in mice has been associated with disturbed metabolism of amino acids (14, 50)
58 and alpha-cell hyperplasia that appears to be mediated by (a) humoral factor(s) secreted from the
59 liver (29, 32), and recent studies suggest that this factor may be increased plasma concentrations of
60 amino acids (12, 24, 41). We hypothesized that a feedback circuitry may exist by which glucagon
61 increases amino acid turnover while amino acids conversely stimulate secretion of glucagon from
62 the pancreas.

63 We therefore initially performed metabolomics analysis of plasma, histology of the pancreas, and
64 protein expression profiles in liver and pancreas tissue from glucagon receptor knockout (*Gcgr*^{-/-})
65 mice in order to dissect the principal components of GR disruption. In addition, we investigated the
66 hepatic clearance of amino acids *in vivo* after prior pharmacological or genetically induced GR
67 blockage. Finally, amino acids were administered to the alpha-cell line α TC1.9 to monitor glucagon
68 secretion and alpha-cell proliferation.

69

70 **Materials and methods**

71 **Animal studies**

72 Animal studies were conducted with permission from the Danish Animal Experiments Inspectorate,
73 Ministry of Environment and Food of Denmark, permit 2013–15–2934–00833, and in accordance
74 with the EU Directive 2010/63/EU and guidelines of Danish legislation governing animal
75 experimentation (1987), and the National Institutes of Health (publication number 85-23). All
76 studies were approved by the local ethical committee.

77 Female C57BL/6JRj mice (12 weeks of age) were obtained from Janvier Labs, Saint-Berthevin
78 Cedex, France. Mice were housed in groups of six to eight in individually ventilated cages and
79 followed a light cycle of 12 hours (lights on 6 am to 6 pm) with ad libitum access to standard chow
80 (catalog no. 1319, Altromin Spezialfutter GmbH & Co, Lage, Germany) and water. Glucagon
81 receptor knockout (*Gcgr*^{-/-}) mice C57BL/6^{Gcgrtm1Mjch} were previously described (14). Male and
82 female homozygotes and wild-type (WT) littermates, age 9-29, weeks were used. During all *Gcgr*^{-/-}
83 and littermate studies, the investigator was blinded to the genotype of the mice in order to avoid
84 bias.

85 **Biochemical and morphometric characterization of *Gcgr*^{-/-} mice**

86 Eleven *Gcgr*^{-/-} mice (six females 18-28 weeks of age and five males 15-25 weeks of age) and 15
87 WT littermates (eight females 18-25 weeks of age and seven males 15-22 weeks of age) were fasted
88 for four hours with free access to water. A 50 µL blood sample was collected from the tail vein, and
89 subsequently the mice were anesthetized with isoflurane (Baxter A/S, Søborg, Denmark). When the
90 mice were sufficiently sedated (absence of reflexes) the abdominal cavity was opened with a
91 midline incision. Tissue samples from the pancreas and liver were harvested and either fixed in
92 formaldehyde 4 % and methanol 1-2 % (Hounisen Laboratory Equipment, Skanderborg, Denmark)

Disruption of glucagon signaling causes hyperaminoacidemia

93 or snap frozen on dry ice. Finally, the mice were subjected to a total blood collection from the
94 inferior vena cava. The blood was immediately transferred to pre-chilled EDTA-coated Eppendorf
95 tubes and stored on ice until centrifuged (1,650 x g, 15 min, 4°C). Plasma was collected and stored
96 in pre-chilled Eppendorf tubes at -20°C until further analysis.

97 **Amino acid clearance in *Gcgr*^{-/-} mice**

98 Seven *Gcgr*^{-/-} mice (six females 9-21 weeks of age and one male 28 weeks of age), and seven WT
99 littermates (six females 9-29 weeks of age and one male 20 weeks of age) were fasted and
100 anesthetized as above and the inferior caval vein exposed. At time 0 min the mice received an
101 injection of 1 µmol/g body weight amino acid mixture, Vamin (Vamin® 14 g/l electrolyte free,
102 catalog no. B05ABA01; Fresenius Kabi, Copenhagen, Denmark, composition of amino acids is
103 shown in table 1), diluted with sterilized phosphate-buffered saline (PBS) to a total volume of 100
104 µL in the caval vein. At time 12 min, the mice were subjected to a total blood collection from the
105 inferior vena cava. Blood samples were handled as described above. Plasma samples were later
106 analyzed for total L-amino acid concentration.

107 **Amino acid clearance after pharmacological disruption of glucagon receptor signaling in mice**

108 Female C57BL/6JRj mice (12 weeks of age) received a glucagon receptor antagonist (GRA, 25–
109 2648, a gift from Novo Nordisk A/S (25)) 180 min prior to the amino acid stimulation experiment.
110 GRA was dissolved in 5% ethanol, 20% propyleneglycol, 10% 2-hydroxypropyl-β-cyclodextrin
111 (vol./vol.) and phosphate buffer at pH 7.5–8.0 to a concentration of 10 mg/mL and administered by
112 oral gavage (100 µL) as a suspension in a dose of 100 mg/kg body weight (42). A control group
113 received 100 µL vehicle. At time 0 min, the tip of the tail was cut and blood glucose concentrations
114 were measured. The mice were then anesthetized with isoflurane, and 1 µmol/g body weight Vamin
115 diluted in sterilized PBS (100 µL) was injected into the inferior vena cava. Control groups received
116 100 µL sterilized PBS. At times 0, 2, 4, 12, or 20 min, the mice were subjected to total blood

Disruption of glucagon signaling causes hyperaminoacidemia

117 collection from the inferior vena cava, and blood glucose concentrations were measured. Blood
118 samples were handled as described above and analyzed for total L-amino acid, insulin, and
119 glucagon concentrations. Clearance was defined as the incremental area under the curve ($iAUC_{0-20}$
120 min).

121 **Amino acid clearance after ligation of the kidneys**

122 Female C57BL/6JRj mice (12 weeks of age) were anesthetized with isoflurane and subsequently
123 subjected to kidney ligation (n=4); four mice were sham operated and served as controls. At time 0
124 min, 1 μ mol/g body weight Vamin diluted in sterilized PBS (100 μ L) was injected into the caval
125 vein. At time 12 min, the mice were subjected to total blood collection from the inferior vena cava.
126 Blood samples were handled as described above and analyzed for total L-amino acid
127 concentrations.

128 **Biochemical analysis**

129 Plasma concentrations of total L-amino acids were quantified using an enzyme-linked
130 immunosorbent assay (ELISA) (catalog no. ab65347; Abcam, Cambridge, UK). This kit determines
131 concentrations of free L-amino acids, but neither protein bound nor D-amino acids. The assay was
132 evaluated by recovery experiments using pooled (n=4) mouse plasma with added known amounts of
133 amino acids (product no. A6282; Sigma Aldrich, Copenhagen, Denmark). Recoveries of amino
134 acids were on average $79\pm 9\%$ in mouse plasma.

135 Plasma concentrations of glucagon were measured using a validated (52) two-site enzyme
136 immunoassay (catalog no.10-1281-01; Mercodia, Upsala, Sweden) according to the manufacturer's
137 protocol.

138 Plasma concentrations of ammonia/ammonium, and bile acids were quantified using enzymatic
139 assays (catalog no. ab83360; Abcam, Cambridge, UK and catalog no. STA-361; Cell Biolabs Inc.,
140 San Diego, USA, resp.).

Disruption of glucagon signaling causes hyperaminoacidemia

141 Plasma concentrations of corticosterone and insulin were quantified using ELISAs (catalog no.
142 ADI-900-097; Enzo, AH diagnostics, Aarhus, Denmark, and catalog no. 10-1247-10; Mercodia AB,
143 Uppsala, Sweden, respectively).

144 In order to avoid bias when performing biochemical analysis all samples were assigned a number,
145 so that genotype and treatment were unknown at the time of analysis.

146 **Plasma Metabolomics**

147 Metabolomic analysis was performed on plasma samples from 11 *Gcgr*^{-/-} (six females 18-28 weeks
148 of age and five males 15-25 weeks of age), and 11 WT littermates (six females 18-25 weeks of age
149 and five males 18-22 weeks of age), also used for biochemical and morphometric characterization.

150 Using liquid chromatographic-triple quadrupole mass spectrometric (LC-MS/MS) measurements
151 and the Absolute*IDQ*TM p180 Kit (BIOCRATES Life Sciences AG, Innsbruck, Austria), 188
152 metabolites were quantified out of 10 µL plasma, including free carnitine, 39 acylcarnitines, 21
153 amino acids, 21 biogenic amines, hexoses, 90 glycerophospholipids (14 lysophosphatidylcholines
154 and 76 phosphatidylcholines), and 15 sphingolipids. The assay procedures of the Absolute*IDQ*TM
155 p180 Kit as well as the metabolite nomenclature have been described in detail previously (40, 54).

156 Sample handling was performed by a Hamilton Microlab STARTM robot (Hamilton Bonaduz AG,
157 Bonaduz, Switzerland) and a Ultravap nitrogen evaporator (Porvair Sciences, Leatherhead, U.K.),
158 besides standard laboratory equipment. Mass spectrometric analyses were done on an API 4000
159 triple quadrupole system (Sciex Deutschland GmbH, Darmstadt, Germany) equipped with a 1200
160 Series HPLC (Agilent Technologies Deutschland GmbH, Böblingen, Germany) and a HTC PAL
161 auto sampler (CTC Analytics, Zwingen, Switzerland) controlled by the software Analyst 1.6.1. Data
162 evaluation for quantification of metabolite concentrations and quality assessment were performed
163 with the software MultiQuant (Sciex) and the Met*IDQ*TM software package, which is an integral

164 part of the Absolute*IDQ*TM Kit. Metabolite concentrations were calculated using internal standards
165 and reported in $\mu\text{mol/L}$.

166 All data has been deposited at Figshare at DOI:10.6084/m9.figshare.5364082.v1
167

168 **Histology and immunohistochemistry**

169 Pancreas and liver tissue samples from the ten *Gcgr*^{-/-} mice (five females 18-25 weeks of age and
170 five males 15-25 weeks of age), and eleven WT littermates (six females 18-25 weeks of age and
171 five males 18-22 weeks of age), also used for plasma metabolomics analysis were fixed for 24
172 hours, and then transferred to 70% ethanol. The tissue samples were embedded in paraffin at the
173 Finsen Laboratory (Rigshospitalet, Copenhagen Biocenter, Copenhagen, Denmark).

174 Tissue sections were stained for insulin (in-house developed guinea pig anti-insulin antibody 2006,
175 1:10000) and glucagon (in-house developed rabbit anti-glucagon 4304, 1:2000). For antigen
176 retrieval, sections were pretreated by boiling in Triethylene glycol (TEG) buffer, pH 9, for 15 min.
177 The sections were then incubated overnight at 4°C with primary antibodies, washed with PBS
178 buffer, pH 7.4, and subsequently incubated with a mixture of Alexa568 labeled donkey-anti rabbit
179 antibody (red, 1:500, Abcam, Cambridge, UK) and Alexa488-labeled goat-anti guinea pig antibody
180 (green, 1:500, Life technologies, Carlsbad, CA, USA). The slides were mounted with DAKO
181 fluorescence mounting medium (Agilent, Santa Clara, CA, USA), and examined using an
182 Axioscope 2 plus microscope (Zeiss, Jena, Germany). Images were taken using CoolSNAP camera
183 (Photometrics, Tucson, AZ, USA).

184 For composition and size, 30 islets from each mouse (two-three sections separated by 200-300 μm
185 evaluated per mouse) were photographed and the relevant areas (insulin, glucagon, and total islet
186 area) were measured using Image-Pro 7 software (Media Cybernetics, Rockville MD, USA) as
187 previously described (31). To measure the mean size of alpha-cells and beta-cells in the two groups
188 of mice, 20 glucagon positive and 20 insulin positive cells were measured for each mouse using

189 Image-Pro 7 software.

190 The pancreas sections were also double-stained for the glucagon-like-peptide-1 receptor (GLP-1R)
191 (mouse GLP-1 receptor antibody 7F38, 1: 200, generous gift from Charles Pyke, Novo Nordisk,
192 Måløv, Denmark) and insulin, glucagon, and somatostatin (in-house developed rabbit somatostatin
193 antibody 1759, 1:4000), respectively. The sections were pretreated with pronase for 10 min (0.1%,
194 firma) at 37°C and incubated overnight with the GLP-1R antibody, and after washing in PBS buffer
195 pH 7.4 subsequently incubated with biotin-anti mouse antibody, 1:200, Vectastain-complex
196 according to the manufacturer's instruction (Vector laboratories, Burlingame, CA, USA), stained
197 with DAB and counterstained lightly with haematoxylin. After this staining was completed, the
198 sections were incubated overnight with either glucagon, insulin or somatostatin antibody and after a
199 wash in PBS, incubated with either Alexa 568 (1:500), or Alexa 488. The slides were then mounted
200 with DAKO fluorescence mounting medium, the sections were examined using Axioscope 2
201 microscope, and images were taken using CoolSNAP camera.

202 **Pancreatic protein extraction and measurements of pancreatic concentrations of glucagon,**
203 **GLP-1, insulin, and somatostatin**

204 Snap-frozen pancreatic tissues from six WT mice (two females 22 and 25 weeks of age and four
205 males 15-20 weeks of age), and five *Gcgr*^{-/-} mice (three females 22-25 weeks of age and two males
206 22 and 25 weeks of age) were subject to peptide extraction carried out as described previously (51).
207 The dipetidyl peptidase-4 (DPP-4) inhibitor, valine-pyrrolidide, was added to all samples and
208 standards (final concentration 0.01 mmol/L) to prevent N-terminal degradation of GLP-1 during the
209 assay incubation. Total amidated GLP-1 concentrations (the sum of 1-36 NH₂, 7-36NH₂, and 9-
210 36NH₂) were quantified using an RIA (codename 89390) specific for the amidated C-terminal of
211 the GLP-1 molecule (35). Active GLP-1 concentrations (7-36 NH₂) were measured using a well-
212 established immunoassay specific for the N-terminus (47). Glucagon concentrations were measured

Disruption of glucagon signaling causes hyperaminoacidemia

213 using an RIA (codename 4305) (18) validated by ELISA (48). Insulin concentrations were
214 measured using an RIA (codename 2006-3) (34). Somatostatin concentrations were measured using
215 an RIA (codename 1758-5) (4).

216 **Stimulation of the alpha-cell line, alphaTC1.9, with amino acids**

217 The alpha-cell line, alphaTC1 Clone 9 (ATCC® CRL-2350™) was used (16). The cells were
218 seeded in 24-well plates (Nunc™, thermo scientific) at a cell density of 4×10^4 per well. Cells 80%
219 confluent were incubated for two hours with PBS (controls) or 1% Vamin added to the media. The
220 cell media were subsequently harvested and centrifuged (1,500 G, 15 min, 4°C,) to remove any
221 cells or debris and kept at -80°C until analysis. For long-term incubation (48 hours) cells were
222 treated with Vamin or PBS as described above and also treated with 5-Bromo-2-DeoxyUridine
223 (BrdU) to assess cell proliferation (catalog no. C10337; Invitrogen, Carlsbad, USA) according to
224 the manufacturer's protocol. Concentrations of glucagon were normalized to total protein content
225 assessed with a BCA kit from Thermo Fisher Scientific (catalog no. 23225).

226 **Statistics**

227 All bioinformatic analyses were done with the Perseus software of the MaxQuant computational
228 platform. For the principal component analysis we included the dataset derived from mass
229 spectrometry and, in addition, all available biochemical data obtained in the current study. A false
230 discovery rate of < 0.05 after Benjamini-Hochberg correction was used in order to correct for
231 multiple testing. When more than two groups were compared, a one-way ANOVA corrected for
232 multiple testing using the Sidak-Holm algorithm was applied. To analyze data from two
233 independent groups un-paired t-test were used. Calculations were made using GraphPad Prism
234 (version 7.02 for Windows; GraphPad Software, La Jolla, CA) and STAT14 (SE) (StataCorp,
235 College station, TX 77845, USA). All data are presented as mean \pm SEM unless otherwise stated.

236

237 **Results**

238 **Biochemical and morphometric characterization of *Gcgr*^{-/-} and WT mice**

239 The body weight of *Gcgr*^{-/-} mice did not differ from WT littermates (31±6 g vs. 30±4 g, P=0.6)
 240 (Fig. 1A). Blood glucose concentrations were lower in *Gcgr*^{-/-} mice compared to WT littermates
 241 (7±1 mmol/L vs. 9±0.8 mmol/L, P<0.0001) (Fig. 1B). Plasma glucagon concentrations were
 242 increased ~20-fold in *Gcgr*^{-/-} mice compared to WT littermates (378±158 pmol/L vs. 21±15 pmol/L,
 243 P<0.0001) (Fig. 1C). Plasma concentrations of total L-amino acids were ~three-fold increased in
 244 *Gcgr*^{-/-} mice compared to WT littermates (7.4±1.4 mmol/L vs. 2.5±0.6 mmol/L, P< 0.0001) (Fig.
 245 1D). Ammonia/ammonium concentrations were increased ~1.5 fold in *Gcgr*^{-/-} mice compared to
 246 WT littermates (27±4 µmol/L vs. 18±4 µmol/L, P=0.0002) (Fig. 1E). Plasma concentrations of
 247 corticosterone and bile acids did not differ between *Gcgr*^{-/-} mice and WT littermates (corticosterone:
 248 176±64 ng/mL vs. 173±100 ng/mL, P=0.9) (Fig. 1F) (bile acids: 6±4 µmol/L vs. 4±0.6 µmol/L,
 249 P=0.3), but the concentration of bile acids showed greater variation in *Gcgr*^{-/-} (Fig. 1G).

250 **Plasma metabolomics analysis**

251 A principle component analysis identified pooled concentrations of amino acids as the primary
 252 component separating *Gcgr*^{-/-} mice from WT littermates (Fig. 2A) and was, furthermore, in an
 253 additional set of analysis, the predictor with most effect (~eight-fold) as well as the most significant
 254 predictor (P=7.7×10⁻⁹) across the 188 identified metabolites (Fig. 2B). Alanine (Ala), glutamine
 255 (Gln), glycine (Gly), threonine (Thr), and serine (Ser) were, listed in decreasing order, the amino
 256 acids found in the highest concentration in *Gcgr*^{-/-} mice (Fig. 2C).

257 ***Gcgr*^{-/-} mice show alpha-cell hyperplasia and hypertrophy**

258 The mean islet size (area) was significantly larger in the *Gcgr*^{-/-} mice compared to WT littermates
 259 (43,206±2,054 µm² vs. 1,1939±697 µm², P<0,0001). In the WT mice, the mean beta-cell area was
 260 5,555±423 µm² amounting to a mean 46% of the mean total islet area, and the mean beta-cell area

261 in the *Gcgr*^{-/-} mice was 7,047±465 μm², amounting to a mean 16% of the total islet area. The
262 percent beta-cell areas was thus smaller in the *Gcgr*^{-/-} mice (P<0.05). In the WT mice, the mean
263 alpha-cell area was 1,150±70 μm² amounting to a mean 10% of the mean total islet area. The mean
264 alpha-cell area in the *Gcgr*^{-/-} mice was 23,013±1,207 μm², corresponding to a mean 53% of the total
265 islet area. The alpha-cell area in the WT mice was significantly smaller than in the *Gcgr*^{-/-} mice
266 (P<0,0001). Representative double stained (insulin and glucagon) pancreatic islets from *Gcgr*^{-/-}
267 mice and WT littermates are shown in Fig. 3A and D. The individual beta-cell size was slightly
268 larger in the *Gcgr*^{-/-} mice than in the WT littermates (142±0.2 μm² vs. 102±0.1 μm², P< 0.001)
269 whereas the mean individual alpha-cell size was much larger in the *Gcgr*^{-/-} mice than in the WT
270 littermates (240±0.3 μm² vs. 87±0.1 μm², P<0.0001).

271 Using a specific antibody against the murine GLP-1 receptor (37), the GLP-1 receptor was
272 identified in pancreatic islets of both WT and *Gcgr*^{-/-} mice. Staining for the GLP-1 receptor,
273 combined with insulin, glucagon, and somatostatin immunohistochemistry, revealed that the GLP-1
274 receptor was localized to the beta-cells in both groups of mice, however, GLP-1 receptor staining of
275 the somatostatin and glucagon producing cells could not be excluded. The GLP-1 receptor was
276 confined to the plasma membrane of insulin positive cells in WT mice whereas in *Gcgr*^{-/-} mice both
277 plasma membrane and cytosolic staining was detected (Fig. 4).

278 **Pancreatic concentrations of glucagon, GLP-1, insulin, and somatostatin in *Gcgr*^{-/-} mice and** 279 **WT littermates**

280 Pancreatic concentrations of extractable glucagon were higher in *Gcgr*^{-/-} mice compared to WT
281 littermates (6,851±2,361 pmol/g vs. 366±285 pmol/g, P=0.0003). Similarly, pancreatic
282 concentrations of extractable, amidated total GLP-1 were significantly higher in *Gcgr*^{-/-} mice
283 compared to WT littermates (388±66 pmol/g vs. 69±56 pmol/g, P<0.0001). Concentrations of
284 active extractable GLP-1 were 63±22 pmol/g in the *Gcgr*^{-/-} mice, whereas active GLP-1 was not

285 detectable in WT littermate pancreata). The analytic detection limit was calculated to be 5 pmol/g.
286 The pancreatic concentrations of extractable insulin did not differ significantly between *Gcgr*^{-/-}
287 mice and WT littermates (5218±1782 pmol/g vs. 7218±676.3 pmol/g, P=0.2). The pancreatic
288 concentration of extractable somatostatin was increased in *Gcgr*^{-/-} mice compared to WT littermates
289 (1,943±231 pmol/g vs. 1,071±91 pmol/g, P=0.002) (data not shown).

290 **Amino acids stimulate glucagon secretion and proliferation of alphaTC1.9 cells**

291 Incubation with amino acids stimulated secretion of glucagon ~six fold from the alphaTC1.9 cells
292 compared with PBS stimulated controls (59±26 pmol/L vs. 9±8 pmol/L, P=0.0006) (Fig. 5A). A
293 prolonged amino acid stimulation of the alphaTC1.9 cells led to an increased proliferation by ~two-
294 fold compared to proliferation of cells not exposed to amino acids (31±8 % vs. 17±4 % BrdU
295 positive cells, P=0.01) (Fig. 5B).

296 **Genetic disruption of glucagon receptor signaling influence on amino acid clearance**

297 *Gcgr*^{-/-} mice and WT littermates received identical amino acid loads (1 µmol/g) at time 0 min. At
298 time 12 min, the plasma Δ amino acid concentration in WT littermates reached 0.8±0.5 mmol/L,
299 whereas the *Gcgr*^{-/-} mice had a Δ concentration of 6±1 mmol/L (data not shown).

300 **The effects of pharmacological blockade of glucagon receptor signaling on amino acid** 301 **clearance in mice**

302 In mice treated with a glucagon receptor antagonist (GRA), fasting plasma concentrations of amino
303 acids tended to be higher than in vehicle treated mice (3.7±0.3 mmol/L vs. 3.0±0.3 mmol/L, P=0.1).
304 In GRA+Vamin treated mice, plasma concentrations of amino acids, at time 12 min, were
305 significantly higher compared to vehicle+Vamin treated mice (9±1 mmol/L vs. 5±1 mmol/L,
306 P=0.006). In the latter group, concentrations returned to near baseline (4.8±0.6 mmol/L) 20 min
307 after the Vamin injection whereas concentrations in GRA+Vamin treated mice remained elevated

308 (7±2 mmol/L) (Fig. 6A). The incremental area under the curve (iAUC_{0-20 min}) was significantly
309 higher in GRA+Vamin treated mice compared to vehicle+Vamin treated mice (P=0.006) (Fig. 6B).

310 **The effects of pharmacological blockade of glucagon receptor signaling on glucagon secretion**
311 **in mice**

312 In GRA treated mice, fasting plasma concentrations of glucagon were significantly higher than in
313 vehicle treated mice (11±1 pmol/L vs. 7±2 pmol/L, P=0.02). Glucagon concentrations increased in
314 Vamin treated groups (vehicle+Vamin and GRA+Vamin). The glucagon response at time 2 min
315 tended to be larger (~two-fold) in GRA treated mice compared to vehicle treated mice (39±11
316 pmol/L vs. 17±4 pmol/L, P=0.1) (Fig. 6C) and the glucagon secretory response was prolonged in
317 GRA treated mice compared to vehicle treated mice (Fig. 6C). The iAUC_{0-20 min} of GRA+Vamin
318 treated mice was four-fold larger when compared to vehicle+Vamin treated mice (82 min×pmol/L
319 vs. 19 min×pmol/L, P=0.02) (Fig. 6D).

320 **The effect of pharmacological blockade of glucagon receptor signaling on insulin secretion in**
321 **mice**

322 Fasting plasma concentrations of insulin did not differ from GRA and vehicle treated mice (0.9±0.2
323 ng/mL vs. 0.6±0.5 ng/mL, P=0.3). Plasma concentrations of insulin increased in response to the
324 amino acid stimulation in both groups. GRA treated mice had a smaller response in insulin secretion
325 compared to vehicle treated mice, although the difference was not significant (13±3 pmol/L vs.
326 19±5 pmol/L, P=0.3) at time 2 min (Fig. 7A). The iAUC_{0-20 min} was smaller (~20 min×ng/mL,
327 P=0.1) in the GRA treated group compared to the vehicle treated group after the amino acid
328 stimulation (Fig. 7B).

329

330

331 **The effect of pharmacological disruption of glucagon receptor signaling on blood glucose**
332 **concentrations in mice**

333 Fasting blood glucose concentrations of GRA and vehicle treated mice differed significantly
334 (6.5 ± 0.2 mmol/L vs. 7.5 ± 0.3 mmol/L, $P=0.008$). Blood glucose concentrations increased in
335 response to the amino acid stimulation in both groups. Blood glucose concentrations also increased
336 in response to PBS in both groups. At time 2 min, the blood glucose levels were significantly lower
337 in GRA+PBS treated mice compared to vehicle+PBS treated mice (8 ± 0.3 mmol/L vs. 11 ± 0.9
338 mmol/L, $P=0.02$) (Fig. 7C). The total area under the curve ($\tau\text{AUC}_{20 \text{ min}}$) was ~two-fold larger in the
339 vehicle+Vamin treated group compared to the GRA+Vamin treated group ($P=0.06$) (Fig. 7D).

340 **Amino acid clearance after ligation of the kidneys**

341 Plasma concentrations of amino acids 12 min after Vamin injection did not differ significantly
342 between mice subjected to ligation of both kidneys and control mice (4.4 ± 0.6 mmol/L vs. 3.7 ± 0.3
343 mmol/L, $P=0.4$) (data not shown).

344

345 **Discussion**

346 Here we demonstrate that normal clearance of amino acids in mice requires glucagon receptor
347 signaling, and that disruption of the latter, by a glucagon receptor antagonist (GRA, 25-2648) or
348 genetic deletion of the glucagon receptor (*Gcgr*^{-/-}), results in significantly higher plasma
349 concentrations of amino acids (hyperaminoacidemia) possibly due to decreased hepatic ureagenesis.

350 Firstly, we *re*-characterized the *Gcgr*^{-/-} mouse with a focus on amino acid metabolism using plasma
351 metabolomics, histology and measurements of pancreatic peptide hormones. As previously reported
352 (11, 14) *Gcgr*^{-/-} mice had lower blood glucose concentrations, elevated plasma concentrations of
353 glucagon, increased alpha-cell mass, increased pancreatic content of glucagon, total - and active -
354 GLP-1, somatostatin, and an equal content of insulin compared to WT littermates. Importantly, we
355 found that *Gcgr*^{-/-} mice had pronounced increases in plasma amino acid and ammonia
356 concentrations. In line with this, a metabolomics driven principal component analysis showed that
357 among 188 metabolites measured after glucagon receptor signaling disruption, the amino acid
358 concentrations showed the most dramatic changes (~41%). In particular, the glucogenic amino acids
359 showed the largest changes. We were, in contrast to what have been reported previously (53),
360 unable to detect significantly higher plasma concentrations of bile acids in *Gcgr*^{-/-} mice compared to
361 WT littermates, but we did observe a greater variability in the *Gcgr*^{-/-} mice and bile acids were
362 indeed higher in some animals. In this report, corticosterone plasma concentrations were found to
363 be similar in *Gcgr*^{-/-} mice and WT mice after a short-term fast (four hours), and others (11, 14) have
364 reported similar corticosterone concentrations under similar conditions. However, the corticosterone
365 levels of *Gcgr*^{-/-} mice were found to be increased two-fold compared to WT mice upon a prolonged
366 fast (>12 hours), suggesting that increased levels of corticosteronemay function to prevent
367 hypoglycemia during prolonged fasting, but are less important in the fed state.

368 Remodeling of the pancreatic islets has been suggested to be of importance for maintaining
369 adequate metabolism and in particular normal glucose concentrations (6).

370 We found the average area of the pancreatic islets to be significantly larger in the *Gcgr*^{-/-} mice than
371 in the WT littermates, in accordance with previous studies (8, 14). The larger alpha-cell area was
372 due to both hyperplasia and hypertrophy, as the individual alpha-cells in the *Gcgr*^{-/-} mice were
373 significantly larger than in WT littermates, and there were also more alpha cells. In the pancreatic
374 alpha-cells, proglucagon is primarily processed to glucagon by pro-hormone convertase (PC) 2 (39),
375 and very little, if any, of proglucagon is processed to GLP-1 (20). Active GLP-1 (7-36NH₂) is
376 therefore *not* a product of the alpha-cell proglucagon processing under normal conditions, according
377 to the present studies. However, we detected significant amounts of fully processed active GLP-1 in
378 pancreatic tissue from *Gcgr*^{-/-} mice. A plasticity in the proglucagon producing cells, may therefore
379 exist, as has previously been reported (19, 39), which be activated upon metabolic or anatomical
380 alterations. However, GLP-1 remained a minor product of proglucagon amounting to only about 1%
381 of glucagon. If active GLP-1 was present in the WT pancreas in the same proportion, the
382 concentration of active GLP-1 would be below detection limit (0.6 pmol/g). The larger amount of
383 active GLP-1 in the pancreas may result in increased concentrations of circulating GLP-1 (14) in
384 *Gcgr*^{-/-} mice, and this has been suggested as an underlying reason for the improved glucose
385 tolerance of these mice (11, 22). In connection with this finding we thought that it would be
386 interesting to investigate the expression of the GLP-1 receptor in the markedly abnormal islets of
387 the *Gcgr*^{-/-} mice compared to the WT littermates. For this we used specific murine GLP-1 receptor
388 antibody (37) but the receptor was found exclusively on the beta-cells. The sensitivity of the
389 immunohistochemical approach does not allow us to exclude expression of a small (and therefore
390 undetectable) number of GLP-1 receptors on the glucagon and somatostatin producing cells, but at
391 least the hyperplastic and hypertrophic alpha-cells do not seem to express the receptor in large

Disruption of glucagon signaling causes hyperaminoacidemia

392 amounts, and expression in the beta-cells was apparently not down regulated by the larger than
393 normal exposure to the ligand. Interestingly, the GLP-1 receptor staining in WT mice was confined
394 to the cell membrane of the beta-cells, whereas both membrane and cytoplasmic staining was found
395 in *Gcgr*^{-/-} islets, due to internalization of the GLP-1 receptor. We speculate that this may be due to
396 increased secretion of pancreatic GLP-1 in the *Gcgr*^{-/-} mice thereby resulting in an increased
397 internalization of the GLP-1 receptor. However, further studies are needed to clarify this.

398 We found an increased density of somatostatin cells in the *Gcgr*^{-/-} islets compared with the WT
399 islets, as also reported in (14) and in accordance with the higher somatostatin content measured in
400 the pancreatic extracts from these mice. The delta-cells may therefore contribute to the increased
401 islet area detected in *Gcgr*^{-/-} mice. Finally, it has been suggested that some alpha-cells, contributing
402 to the hyperplasia, may transdifferentiate to beta-cells (30, 44). Our data showed, as reported in (14)
403 that the pancreatic insulin content did not differ significantly between *Gcgr*^{-/-} mice and WT
404 littermates. However, insulin immunostaining showed a slightly larger beta-cell area in *Gcgr*^{-/-} mice
405 than in WT littermates.

406 GRA treated WT mice had reduced clearance of an intravenous load of mixed amino acids,
407 compared to vehicle treated mice suggesting that intact glucagon receptor signaling is required for
408 adequate clearance of exogenous amino acids. Both groups responded with an increase in glucagon
409 concentrations upon amino acid stimulation. However, the glucagon increase was larger in GRA
410 treated mice compared to vehicle treated mice. The greater and longer lasting glucagon response
411 observed in GRA treated mice might be due to the persistently higher level of amino acids in GRA
412 treated mice. Both groups responded with an increase in insulin concentrations upon amino acid
413 stimulation. However, a tendency to a decreased insulin response in GRA treated mice was
414 observed, perhaps due to GRA inhibition of glucagon-induced insulin secretion (15, 23).

Disruption of glucagon signaling causes hyperaminoacidemia

415 In the *Gcgr*^{-/-} mice, the receptor deletion can lead to lifelong metabolic adaptations. These adaptations
416 may skew the results, and make the results from the model difficult to interpret in terms of
417 physiology and less relevant for the understanding of human metabolic disease (8). However, we
418 were able to demonstrate decreased clearance of amino acids using both *Gcgr*^{-/-} as well as a highly
419 specific glucagon receptor antagonist. It is therefore unlikely that the decreased clearance of amino
420 acids is a result of biological adaptation following knockout of the glucagon receptor gene.
421 Furthermore, the glucagon receptor is not expressed in human or mouse adipose tissue or in muscles
422 (there is a single aberrant report of receptor expression in muscles (17), and we were also able to
423 demonstrate that ligation of the kidneys did not acutely influence amino acid clearance in WT mice.
424 We therefore suggest that the observed effects of glucagon receptor blockade on amino acid
425 metabolism are a consequence of disrupted glucagon signaling in the liver.

426 Cultured alpha cells (alphaTC1.9) incubated with amino acids showed increased proliferation and
427 glucagon secretion, supporting a role for amino acids as growth factors for the alpha-cells (32, 41)
428 and as stimulators of glucagon secretion as previously suggested (3, 26, 36, 38, 41, 45).

429 The amino acid clearance experiments were performed using mice anesthetized with isoflurane.
430 Isoflurane has, in contrast to other rodent anesthetics, previously been shown *not* to attenuate
431 arginine-stimulated glucagon secretion in mice (52), supporting that the glucagon responses
432 observed are physiologically relevant. The use of anesthetized mice allowed us to obtain sufficient
433 plasma to perform accurate measurements of amino acids, glucagon, and insulin. In addition, by
434 using anesthetized mice we were also able to exclude the effects of muscular contractions on
435 plasma amino acids (46).

436 Some of the findings in *Gcgr*^{-/-} mice are reflected in human studies: patients with inactivating
437 glucagon receptor knockout mutations show pancreatic swelling, hyperaminoacidemia, and

Disruption of glucagon signaling causes hyperaminoacidemia

438 hyperglucagonemia (27). Subjects with non-alcoholic fatty liver disease (NAFLD) and type 2
439 diabetes have been shown to have elevated concentrations of plasma amino acids and
440 hyperglucagonemia (49). These findings suggest that, also in humans, impaired liver function leads
441 to hyperglucagonemia, perhaps as a consequence of impaired glucagon action on hepatic amino
442 acid turnover, leading to elevated concentrations of circulating amino acids that stimulate alpha-
443 cells. In line with this, patients with glucagon producing tumors (glucagonomas) show
444 hypoaminoacidemia (9, 50). This may be caused by the high rate of glucagon accelerated hepatic
445 amino acid turnover and ureagenesis.

446 In conclusion, both pharmacological and genetic disruption of glucagon receptor signaling leads to
447 severely impaired amino acid clearance in mice, supporting an essential role for glucagon receptor
448 signaling in acute amino acid turnover in mice. Furthermore, mice lacking glucagon receptor
449 signaling (*Gcgr*^{-/-} mice) have hyperaminoacidemia, hyperglucagonemia, and alpha-cell hyperplasia.
450 These findings support the existence of a liver - alpha-cell axis with amino acid and glucagon
451 feedback loops in mice. This feedback circuitry may be particularly important during ingestion of
452 protein rich meals that raise the concentration of circulating amino acids. Disruption of the axis, be
453 it by liver dysfunction as seen in NAFLD patients or in defects in glucagon receptor signaling as
454 seen in patients with inactivating glucagon receptor mutations or treatment with a glucagon receptor
455 antagonist, leads to hyperaminoacidemia and is, in this way, responsible for the apparent
456 hypersecretion of glucagon (hyperglucagonemia) rather than disturbances in glucose metabolism.

457

458

459

460

461

462

463 **Acknowledgement**

464 We thank Julia Silke Becker for metabolomics measurements performed at the Helmholtz Zentrum
465 München, Genome Analysis Center, Metabolomics Core Facility and the Finsen Core Laboratory
466 (Biotech Research & Innovation Centre, Copenhagen, Denmark). We are very grateful for the help
467 of the laboratory technician Ramaya Kweder and Associate Professor Reidar Albrechtsen (Biotech
468 Research and Innovation Centre (BRIC), University of Copenhagen, Denmark) with cell
469 proliferation assays.

470

471 **Funding**

472 This study was supported by the Novo Nordisk Foundation (NNF) Center for Basic Metabolic
473 Research University of Copenhagen, NNF application number: 13563, EliteForsk Rejsestipendiat
474 (2016), The Danish Council for independent research (DFF-1333-00206A), The Augustinus
475 Foundation, Aase and Ejnar Danielsens Foundation, The Mærsk Foundation, The Holger Rabitz
476 Foundation, Doctor Johannes Nicolaj Krogsgaard and wife Else Krogsgaard memorial-scholarship
477 for medical research and medical students at the university of Copenhagen, European Biology
478 Organization (EMBO) and the European Foundation For the study of Diabetes (EFSD), Novo
479 Scholarship programme 2017, and by a grant from the German Federal Ministry of Education and
480 Research (BMBF) to the German Center Diabetes Research (DZD e.V.),

481

482 **Disclosure**

483 No conflicts of interest, financial or otherwise, are declared by the authors.

484

485

486 **Author contributions**

487 Conceived and designed research: K.D.G., J.P., N.J.W.A. and J.J.H. Performed experiments:
488 K.D.G., M.W.S., C.Ø., H.K., S.S.P, C.P., J.A., S.L.J., B.H., J.H., J.P., and N.J.W.A., Analyzed data:
489 K.D.G., M.W.S., C.Ø., S.S.P., J.A., J.P., N.J.W.A., and J.J.H. Interpreted results of experiments:
490 K.D.G., M.W.S., C.Ø., H.K., S.S.P, H.V., J.P., N.J.W.A., and J.J.H. Prepared figures: K.D.G., and
491 N.J.W.A. Drafted manuscript: K.D.G. and N.J.W.A. Edited and revised manuscript: M.W.S., C.Ø.,
492 H.K., S.S.P., H.V., B.H., M.J.C., J.P., and J.J.H.. Approved final version of manuscript: K.D.G.,
493 M.W.S., C.Ø., H.K., S.S.P., H.V., C.P., J.A., S.L.J., B.H., J.H., M.J.C., J.P., N.J.W.A., and J.J.H..

494

495

496

497

498 **References**

- 499 1. **Alford FP, Bloom SR, Nabarro JD, Hall R, Besser GM, Coy DH, Kastin AJ, and Schally**
500 **AV.** Glucagon control of fasting glucose in man. *Lancet (London, England)* 2: 974-977, 1974.
- 501 2. **Almdal TP, Jensen T, and Vilstrup H.** Increased hepatic efficacy of urea synthesis from
502 alanine in insulin-dependent diabetes mellitus. *European journal of clinical investigation* 20: 29-34, 1990.
- 503 3. **Assan R, Attali JR, Ballerio G, Boillot J, and Girard JR.** Glucagon secretion induced by
504 natural and artificial amino acids in the perfused rat pancreas. *Diabetes* 26: 300-307, 1977.
- 505 4. **Bersani M, Johnsen AH, and Holst JJ.** Oxidation/reduction explains heterogeneity of
506 pancreatic somatostatin. *FEBS letters* 279: 237-239, 1991.
- 507 5. **Boden G, Rezvani I, and Owen OE.** Effects of glucagon on plasma amino acids. *The*
508 *Journal of clinical investigation* 73: 785-793, 1984.
- 509 6. **Chambers AP, Sorrell JE, Haller A, Roelofs K, Hutch CR, Kim KS, Gutierrez-Aguilar**
510 **R, Li B, Drucker DJ, D'Alessio DA, Seeley RJ, and Sandoval DA.** The Role of Pancreatic Proglucagon
511 in Glucose Homeostasis in Mice. *Cell metabolism* 25: 927-934.e923, 2017.
- 512 7. **Charlton MR, Adey DB, and Nair KS.** Evidence for a catabolic role of glucagon during an
513 amino acid load. *J Clin Invest* 98: 90-99, 1996.
- 514 8. **Charron MJ, and Vuguin PM.** Lack of glucagon receptor signaling and its implications
515 beyond glucose homeostasis. *The Journal of endocrinology* 224: R123-130, 2015.
- 516 9. **Chastain MA.** The glucagonoma syndrome: a review of its features and discussion of new
517 perspectives. *Am J Med Sci* 321: 306-320, 2001.
- 518 10. **Cherrington AD, Chiasson JL, Liljenquist JE, Lacy WW, and Park CR.** Control of
519 hepatic glucose output by glucagon and insulin in the intact dog. *Biochem Soc Symp* 31-45, 1978.
- 520 11. **Conarello SL, Jiang G, Mu J, Li Z, Woods J, Zychband E, Ronan J, Liu F, Roy RS, Zhu**
521 **L, Charron MJ, and Zhang BB.** Glucagon receptor knockout mice are resistant to diet-induced obesity and
522 streptozotocin-mediated beta cell loss and hyperglycaemia. *Diabetologia* 50: 142-150, 2007.
- 523 12. **Dean ED, Li M, Prasad N, Wisniewski SN, Von Deylen A, Spaeth J, Maddison L, Botros**
524 **A, Sedgeman LR, Bozadjieva N, Ilkayeva O, Coldren A, Poffenberger G, Shostak A, Semich MC,**
525 **Aamodt KI, Phillips N, Yan H, Bernal-Mizrachi E, Corbin JD, Vickers KC, Levy SE, Dai C, Newgard**
526 **C, Gu W, Stein R, Chen W, and Powers AC.** Interrupted Glucagon Signaling Reveals Hepatic alpha-cell
527 Axis and Role for L-Glutamine in alpha-cell Proliferation. *Cell metabolism* 25: 1362-1373.e1365, 2017.
- 528 13. **Flakoll PJ, Borel MJ, Wentzel LS, Williams PE, Lacy DB, and Abumrad NN.** The role of
529 glucagon in the control of protein and amino acid metabolism in vivo. *Metabolism: clinical and experimental*
530 43: 1509-1516, 1994.
- 531 14. **Gelling RW, Du XQ, Dichmann DS, Romer J, Huang H, Cui L, Obici S, Tang B, Holst**
532 **JJ, Fledelius C, Johansen PB, Rossetti L, Jelicks LA, Serup P, Nishimura E, and Charron MJ.** Lower
533 blood glucose, hyperglucagonemia, and pancreatic alpha cell hyperplasia in glucagon receptor knockout
534 mice. *Proceedings of the National Academy of Sciences of the United States of America* 100: 1438-1443,
535 2003.
- 536 15. **Goldfine ID, Cerasi E, and Luft R.** Glucagon stimulation of insulin release in man:
537 inhibition during hypoglycemia. *The Journal of clinical endocrinology and metabolism* 35: 312-315, 1972.
- 538 16. **Hamaguchi K, and Leiter EH.** Comparison of cytokine effects on mouse pancreatic alpha-
539 cell and beta-cell lines. Viability, secretory function, and MHC antigen expression. *Diabetes* 39: 415-425,
540 1990.
- 541 17. **Hansen LH, Abrahamsen N, and Nishimura E.** Glucagon receptor mRNA distribution in
542 rat tissues. *Peptides* 16: 1163-1166, 1995.
- 543 18. **Holst JJ.** Evidence that glicentin contains the entire sequence of glucagon. *The Biochemical*
544 *journal* 187: 337-343, 1980.
- 545 19. **Holst JJ.** Molecular heterogeneity of glucagon in normal subjects and in patients with
546 glucagon-producing tumours. *Diabetologia* 24: 359-365, 1983.
- 547 20. **Holst JJ, Bersani M, Johnsen AH, Kofod H, Hartmann B, and Orskov C.** Proglucagon
548 processing in porcine and human pancreas. *The Journal of biological chemistry* 269: 18827-18833, 1994.

- 549 21. **Holst JJ, Wewer Albrechtsen NJ, Pedersen J, and Knop FK.** Glucagon and Amino Acids
550 Are Linked in a Mutual Feedback Cycle: The Liver-alpha-Cell Axis. *Diabetes* 66: 235-240, 2017.
- 551 22. **Jun LS, Millican RL, Hawkins ED, Konkol DL, Showalter AD, Christe ME, Michael
552 MD, and Sloop KW.** Absence of glucagon and insulin action reveals a role for the GLP-1 receptor in
553 endogenous glucose production. *Diabetes* 64: 819-827, 2015.
- 554 23. **Kawai K, Yokota C, Ohashi S, Watanabe Y, and Yamashita K.** Evidence that glucagon
555 stimulates insulin secretion through its own receptor in rats. *Diabetologia* 38: 274-276, 1995.
- 556 24. **Kim J, Okamoto H, Huang Z, Anguiano G, Chen S, Liu Q, Cavino K, Xin Y, Na E,
557 Hamid R, Lee J, Zambrowicz B, Unger R, Murphy AJ, Xu Y, Yancopoulos GD, Li W-h, and Gromada
558 J.** Amino Acid Transporter Slc38a5 Controls Glucagon Receptor Inhibition-Induced Pancreatic Alpha-Cell
559 Hyperplasia in Mice. *Cell metabolism* 25: 1348-1361.e1348, 2017.
- 560 25. **Kodra JT, Jorgensen AS, Andersen B, Behrens C, Brand CL, Christensen IT,
561 Guldbrandt M, Jeppesen CB, Knudsen LB, Madsen P, Nishimura E, Sams C, Sidelmann UG,
562 Pedersen RA, Lynn FC, and Lau J.** Novel glucagon receptor antagonists with improved selectivity over
563 the glucose-dependent insulinotropic polypeptide receptor. *J Med Chem* 51: 5387-5396, 2008.
- 564 26. **Kuhara T, Ikeda S, Ohneda A, and Sasaki Y.** Effects of intravenous infusion of 17 amino
565 acids on the secretion of GH, glucagon, and insulin in sheep. *The American journal of physiology* 260: E21-
566 26, 1991.
- 567 27. **Larger E, Wewer Albrechtsen NJ, Hansen LH, Gelling RW, Capeau J, Deacon CF,
568 Madsen OD, Yakushiji F, De Meyts P, Holst JJ, and Nishimura E.** Pancreatic alpha-cell hyperplasia and
569 hyperglucagonemia due to a glucagon receptor splice mutation. *Endocrinology, diabetes & metabolism case
570 reports* Epub: 2016.
- 571 28. **Liljenquist JE, Chiassan JL, Cherrington AD, Keller U, Jennings AS, Bomboy JD, and
572 Lacy WW.** An important role for glucagon in the regulation of glucose production in vivo. *Metabolism:
573 clinical and experimental* 25: 1371-1373, 1976.
- 574 29. **Longuet C, Robledo AM, Dean ED, Dai C, Ali S, McGuinness I, de Chavez V, Vuguin
575 PM, Charron MJ, Powers AC, and Drucker DJ.** Liver-specific disruption of the murine glucagon receptor
576 produces alpha-cell hyperplasia: evidence for a circulating alpha-cell growth factor. *Diabetes* 62: 1196-1205,
577 2013.
- 578 30. **Lysy PA, Weir GC, and Bonner-Weir S.** Making beta cells from adult cells within the
579 pancreas. *Curr Diab Rep* 13: 695-703, 2013.
- 580 31. **Merino B, Alonso-Magdalena P, Lluesma M, Neco P, Gonzalez A, Marroqui L, Garcia-
581 Arevalo M, Nadal A, and Quesada I.** Pancreatic alpha-cells from female mice undergo morphofunctional
582 changes during compensatory adaptations of the endocrine pancreas to diet-induced obesity. *Scientific
583 reports* 5: 11622, 2015.
- 584 32. **Morley MG, Leiter EH, Eisenstein AB, and Strack I.** Dietary modulation of alpha-cell
585 volume and function in strain 129/J mice. *The American journal of physiology* 242: G354-359, 1982.
- 586 33. **Muller WA, Faloona GR, Aguilar-Parada E, and Unger RH.** Abnormal alpha-cell function
587 in diabetes. Response to carbohydrate and protein ingestion. *The New England journal of medicine* 283: 109-
588 115, 1970.
- 589 34. **Orskov C, Jeppesen J, Madsbad S, and Holst JJ.** Proglucagon products in plasma of
590 noninsulin-dependent diabetics and nondiabetic controls in the fasting state and after oral glucose and
591 intravenous arginine. *J Clin Invest* 87: 415-423, 1991.
- 592 35. **Orskov C, Rabenhøj L, Wettergren A, Kofod H, and Holst JJ.** Tissue and plasma
593 concentrations of amidated and glycine-extended glucagon-like peptide I in humans. *Diabetes* 43: 535-539,
594 1994.
- 595 36. **Pipeleers DG, Schuit FC, Van Schravendijk CF, and Van de Winkel M.** Interplay of
596 nutrients and hormones in the regulation of glucagon release. *Endocrinology* 117: 817-823, 1985.
- 597 37. **Pyke C, Heller RS, Kirk RK, Ørskov C, Reedtz-Runge S, Kaastrup P, Hvelplund A,
598 Bardram L, Calatayud D, and Knudsen LB.** GLP-1 Receptor Localization in Monkey and Human Tissue:
599 Novel Distribution Revealed With Extensively Validated Monoclonal Antibody. *Endocrinology* 155: 1280-
600 1290, 2014.

- 601 38. **Rocha DM, Faloona GR, and Unger RH.** Glucagon-stimulating activity of 20 amino acids
602 in dogs. *J Clin Invest* 51: 2346-2351, 1972.
- 603 39. **Rouille Y, Westermark G, Martin SK, and Steiner DF.** Proglucagon is processed to
604 glucagon by prohormone convertase PC2 in alpha TC1-6 cells. *Proceedings of the National Academy of*
605 *Sciences of the United States of America* 91: 3242-3246, 1994.
- 606 40. **Römisch-Margl W, Prehn C, Bogumil R, Röhring C, Suhre K, and Adamski J.** Procedure
607 for tissue sample preparation and metabolite extraction for high-throughput targeted metabolomics.
608 *Metabolomics* 8: 133-142, 2012.
- 609 41. **Solloway MJ, Madjidi A, Gu C, Eastham-Anderson J, Clarke HJ, Kljavin N, Zavala-**
610 **Solorio J, Kates L, Friedman B, Brauer M, Wang J, Fiehn O, Kolumam G, Stern H, Lowe JB,**
611 **Peterson AS, and Allan BB.** Glucagon Couples Hepatic Amino Acid Catabolism to mTOR-Dependent
612 Regulation of alpha-Cell Mass. *Cell Rep* 12: 495-510, 2015.
- 613 42. **Steenberg VR, Jensen SM, Pedersen J, Madsen AN, Windelov JA, Holst B, Quistorff B,**
614 **Poulsen SS, and Holst JJ.** Acute disruption of glucagon secretion or action does not improve glucose
615 tolerance in an insulin-deficient mouse model of diabetes. *Diabetologia* 59: 363-370, 2016.
- 616 43. **Taborsky GJ, Jr.** The physiology of glucagon. *Journal of diabetes science and technology* 4:
617 1338-1344, 2010.
- 618 44. **Thorel F, Nepote V, Avril I, Kohno K, Desgraz R, Chera S, and Herrera PL.** Conversion
619 of adult pancreatic alpha-cells to beta-cells after extreme beta-cell loss. *Nature* 464: 1149-1154, 2010.
- 620 45. **Unger RH, Ohneda A, Aguilar-Parada E, and Eisentraut AM.** The role of aminogenic
621 glucagon secretion in blood glucose homeostasis. *The Journal of clinical investigation* 48: 810-822, 1969.
- 622 46. **Wagenmakers AJ.** Muscle amino acid metabolism at rest and during exercise: role in human
623 physiology and metabolism. *Exerc Sport Sci Rev* 26: 287-314, 1998.
- 624 47. **Wewer Albrechtsen NJ, Bak MJ, Hartmann B, Christensen LW, Kuhre RE, Deacon CF,**
625 **and Holst JJ.** Stability of glucagon-like peptide 1 and glucagon in human plasma. *Endocr Connect* 4: 50-57,
626 2015.
- 627 48. **Wewer Albrechtsen NJ, Hartmann B, Veedfald S, Windelov JA, Plamboeck A, Bojsen-**
628 **Moller KN, Idorn T, Feldt-Rasmussen B, Knop FK, Vilsboll T, Madsbad S, Deacon CF, and Holst JJ.**
629 Hyperglucagonaemia analysed by glucagon sandwich ELISA: nonspecific interference or truly elevated
630 levels? *Diabetologia* 57: 1919-1926, 2014.
- 631 49. **Wewer Albrechtsen NJ, Junker AE, Galsgaard KD, Holst JJ, Knop FK, and Vilsbøll T.**
632 Fasting Levels of Amino Acids Are Correlated to Hyperglucagonemia in Patients with Nonalcoholic Fatty
633 Liver Disease Independently of Type 2 Diabetes. In: *American Diabetes Association, Association's 77th*
634 *Scientific Sessions Abstract Book*. San Diego, California 2017.
- 635 50. **Wewer Albrechtsen NJ, Kuhre RE, Pedersen J, Knop FK, and Holst JJ.** The biology of
636 glucagon and the consequences of hyperglucagonemia. *Biomarkers in medicine* 10: 1141-1151, 2016.
- 637 51. **Wewer Albrechtsen NJ, Kuhre RE, Torang S, and Holst JJ.** The intestinal distribution
638 pattern of appetite- and glucose regulatory peptides in mice, rats and pigs. *BMC research notes* 9: 60, 2016.
- 639 52. **Wewer Albrechtsen NJ, Kuhre RE, Windelov JA, Orgaard A, Deacon CF, Kissow H,**
640 **Hartmann B, and Holst JJ.** Dynamics of glucagon secretion in mice and rats revealed using a validated
641 sandwich ELISA for small sample volumes. *American journal of physiology Endocrinology and metabolism*
642 311: E302-309, 2016.
- 643 53. **Yang J, MacDougall ML, McDowell MT, Xi L, Wei R, Zavadoski WJ, Molloy MP,**
644 **Baker JD, Kuhn M, Cabrera O, and Treadway JL.** Polyomic profiling reveals significant hepatic
645 metabolic alterations in glucagon-receptor (GCGR) knockout mice: implications on anti-glucagon therapies
646 for diabetes. *BMC Genomics* 12: 281, 2011.
- 647 54. **Zukunft S, Sorgenfrei M, Prehn C, Möller G, and Adamski J.** Targeted Metabolomics of
648 Dried Blood Spot Extracts. *Chromatographia* 76: 1295-1305, 2013.

649 **Figure captions and legends**

650 **Fig. 1:** Biochemical characterization of glucagon receptor knockout mice and wild-type littermates

651 (A) The body weight of glucagon receptor knockout mice (*Gcgr*^{-/-}) male (red empty circles) or
652 female mice (red full circles) did not differ significantly, P=0.4, from wild-type (WT) male (black
653 empty squares) or female littermates (black full squares). The body weight of female *Gcgr*^{-/-} did not
654 differ from *Gcgr*^{-/-} males (P=0.2). The body weight of female WT differed from WT males (25±3 g
655 vs. 33±5 g, P=0.0002). (B) Blood glucose concentrations in *Gcgr*^{-/-} mice were significantly lower
656 compared to WT, P<0.0001, and did not differ between males and females. (C) Plasma
657 concentrations of glucagon were significantly increased in *Gcgr*^{-/-} mice compared to WT, P<0.0001,
658 and did not differ between males and females. (D) Plasma amino acid concentrations were
659 significantly increased in *Gcgr*^{-/-} mice compared to WT, P<0.0001, and did not differ between
660 males and females. (E) Plasma ammonia/ammonium concentrations were significantly increased in
661 *Gcgr*^{-/-} mice compared to WT, P=0.0002, and did not differ between males and females. (F) Plasma
662 concentrations of corticosterone did not differ between *Gcgr*^{-/-} mice and WT, P=0.8. Plasma
663 corticosterone concentrations of *Gcgr*^{-/-} females did not differ from *Gcgr*^{-/-} males, P=0.2. Plasma
664 corticosterone concentrations of WT females differed from WT males (251±72 ng/mL vs. 85±25
665 ng/mL, P<0.0001). (G) Plasma concentrations of bile acids did not differ between *Gcgr*^{-/-} mice and
666 WT, P=0.3, and did not differ between males and females. *Gcgr*^{-/-} mice n=11 (15-28 weeks of age),
667 WT littermates n= 15 (15-25 weeks of age). Data is presented as mean±SD, *****P < 0.0001.

668

669

670 **Fig. 2:** Glucagon receptor knockout mice show hyperaminoacidemia

671 (A) A principal component analysis revealed that plasma amino acid concentrations (component 1)
672 separated glucagon receptor knockout mice (*Gcgr*^{-/-}) and wild-type (WT) littermates completely.

673 (B) A principal component analysis revealed that amino acids (red dot) were the principal
674 component showing the greatest difference when *Gcgr*^{-/-} mice were compared to WT littermates.

675 Green dots indicate the metabolites that were significantly increased in *Gcgr*^{-/-} compared to WT
676 littermates, blue dots indicate metabolites that were significantly decreased in *Gcgr*^{-/-} compared to

677 WT littermates. (C) In *Gcgr*^{-/-} mice the concentrations of certain amino acids were elevated to a
678 larger degree than those of other amino acids. All amino acid concentrations, except the

679 concentration of tryptophan (Trp), were significantly higher in *Gcgr*^{-/-} mice (red bars) compared to
680 WT littermates (black bars). Data presented as mean±SEM. *Gcgr*^{-/-} mice n=11 (15-28 weeks of

681 age), WT littermates n=11 (18-25 weeks of age).

682

683

684 **Fig. 3.** Glucagon receptor knockout mice show alpha-cell hyperplasia and hypertrophy

685 (A) A typical immunohistochemical staining for glucagon (red, B) and insulin (green, C) in
686 glucagon receptor knockout (*Gcgr*^{-/-}) mice. (D) A typical immunohistochemical staining for
687 glucagon (red, E) and insulin (green, F) in wild-type (WT) littermates. The dotted arrows indicate a
688 glucagon positive cell and the solid arrows indicate an insulin positive cell, the *Gcgr*^{-/-} mice showed
689 an increased size of glucagon positive cells compared to WT littermates. All images are shown at
690 X200 magnification. The scale bar indicates 50 μm.

691

692 **Fig. 4:** Glucagon receptor knockout mice show an internalization of the glucagon-like-peptide-1
693 receptor compared to wild-type littermates

694 (A) A typical insulin staining pattern in wild-type (WT) littermates and (C) in glucagon receptor
695 knockout (*Gcgr*^{-/-}) mice. (B) A typical glucagon-like-peptide-1 (GLP-1) receptor staining pattern in
696 WT littermates and (D, F, H) in *Gcgr*^{-/-} mice. (E) A typical somatostatin and (G) glucagon staining
697 pattern in *Gcgr*^{-/-} mice. The arrows (in A, B, C and D) indicate cells that stain positive for both
698 insulin and the GLP-1 receptor. GLP-1 receptor staining was localized to insulin positive cells in
699 both WT and *Gcgr*^{-/-} mice. The GLP-1 receptor staining was confined to the plasma membrane in
700 WT mice whereas both membrane and cytosolic staining was observed in *Gcgr*^{-/-} mice. All images
701 are shown at X200 magnification. The scale bar indicates 50 μm.

702

703

704 **Fig. 5:** Amino acids stimulate proliferation and secretion in cultured alpha-cells

705 (A) The cultured alphaTC1.9 cells stimulated four hours with Vamin (1 %) (red circles) showed a
706 significant increase in glucagon secretion compared to PBS stimulated control cells (black squares).

707 (B) The alphaTC1.9 cells stimulated 48 hours with Vamin (red circles) showed an increased
708 proliferation compared to control cells stimulated with phosphate-buffered saline (PBS) (black
709 squares). Data presented as mean±SD, *P < 0.05, ***P < 0.001.

710 **Fig. 6:** Total L-Amino acids and glucagon plasma concentrations following amino acid stimulation
711 during pharmacological blockade of the glucagon receptor

712 (A) Mice treated with the glucagon receptor antagonist (GRA) (red line and circles) were not able
713 to clear the amino acid load (Vamin, 1 $\mu\text{mol/g}$ body weight) administered at time 0 min whereas
714 mice treated with vehicle (blue line and upwards triangles) almost completely cleared the same
715 amino acid load within 12 min. The control groups receiving phosphate-buffered saline (PBS)
716 instead of Vamin after GRA treatment (pink line and squares) or vehicle administration (light blue
717 line and downwards triangles) showed no acute changes in the concentration of amino acids. (B)
718 The incremental areas under the curve (iAUC_{0-20 min}) are shown for the four groups. (C) Mice
719 treated with GRA responded to the amino acid stimulation with a larger increase in glucagon
720 concentrations compared to mice treated with vehicle. The controls groups receiving PBS after
721 GRA or vehicle treatment showed no change in glucagon concentrations. (D) The iAUC_{0-20 min} are
722 shown for the four groups. Data presented as mean \pm SEM (n=3-7), *P < 0.05, **P < 0.01.

723

724

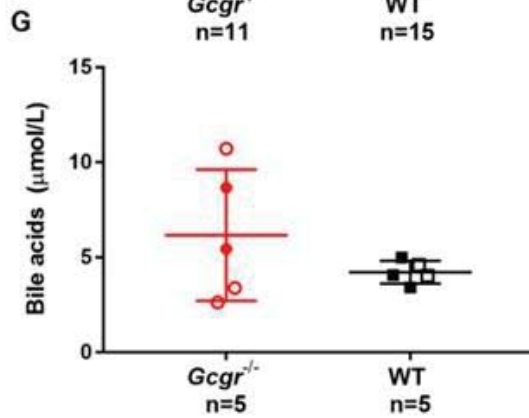
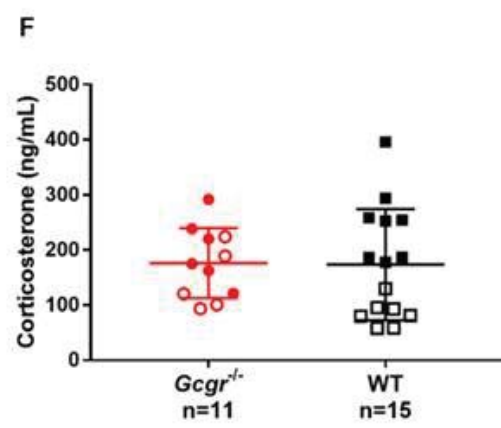
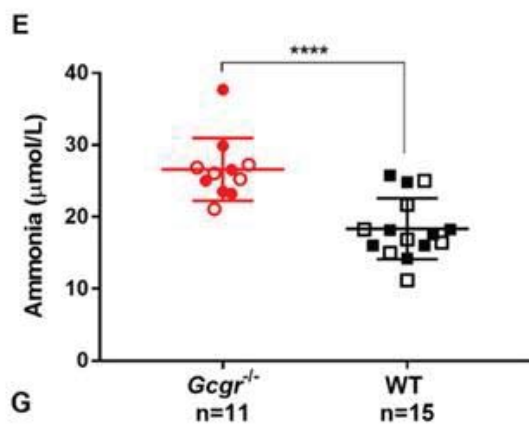
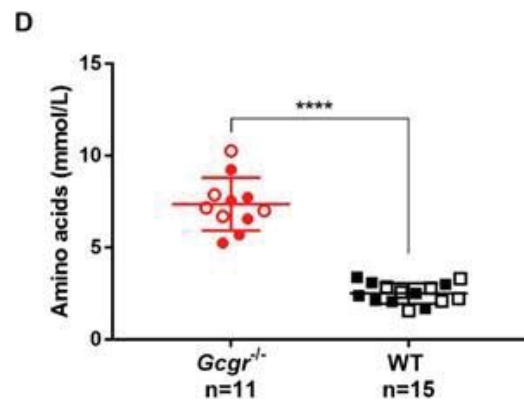
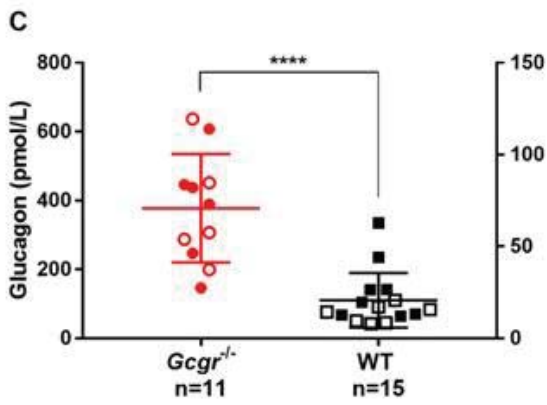
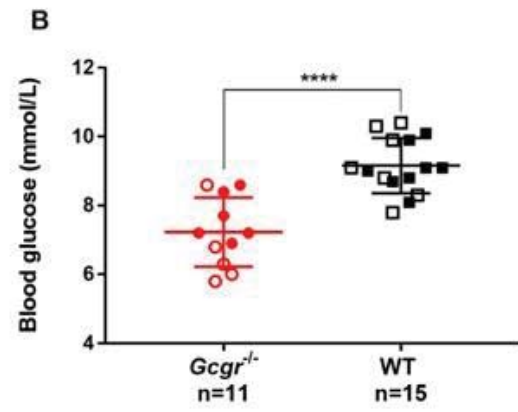
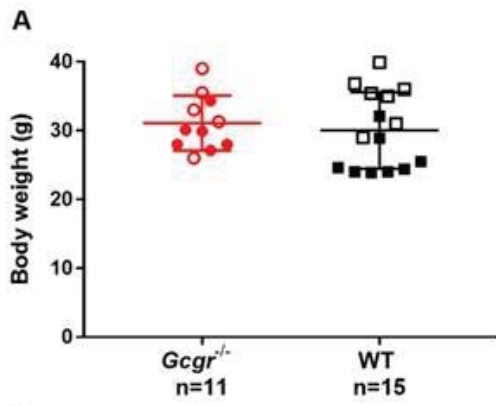
725 **Fig. 7:** Plasma insulin and blood glucose concentrations following amino acid stimulation during
726 pharmacological disruption of the glucagon receptor

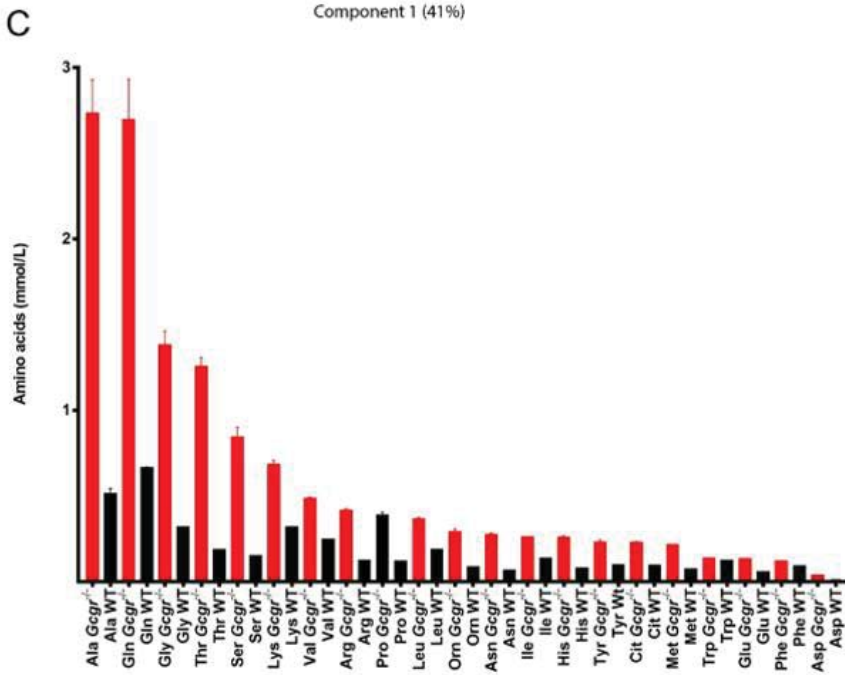
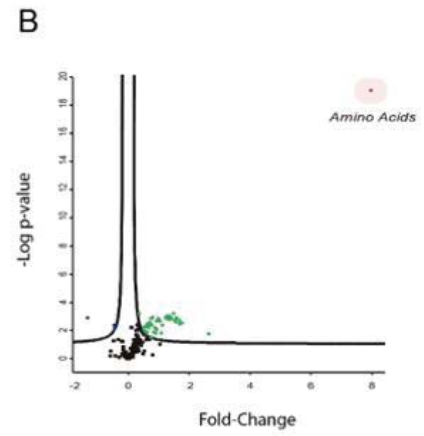
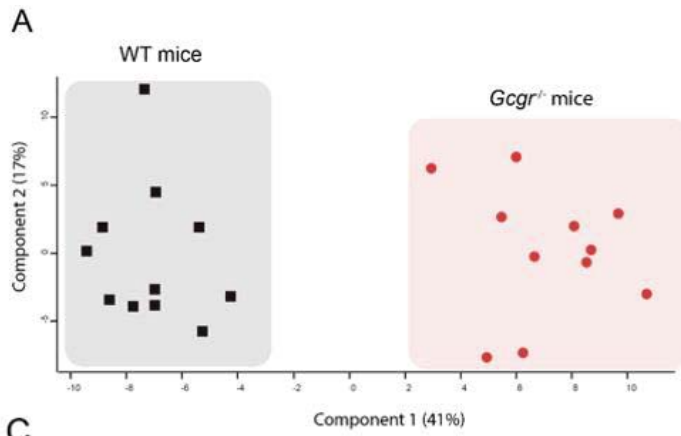
727 (A) Both glucagon receptor antagonist (GRA, red line and circles) and vehicle (blue line and
728 upward triangles) treated mice responded with a fast increase in plasma insulin concentration
729 following amino acid infusion (Vamin, 1 $\mu\text{mol/g}$ body weight). Control groups receiving
730 phosphate-buffered saline (PBS) instead of amino acids (GRA+PBS, pink line and squares, and
731 vehicle+PBS, light blue line and downward triangles) showed no change in insulin concentrations.
732 (B) The incremental areas under the curve ($i\text{AUC}_{0-20 \text{ min}}$) are shown for the four groups. The amino
733 acid stimulation resulted in an increase in insulin concentrations in both groups. (C) Blood glucose
734 concentrations increased in response to the amino acid stimulation in both groups. Blood glucose
735 concentrations also increased in the control groups receiving PBS. (D) The total area under the
736 curve ($\text{T}\text{AUC}_{0-20 \text{ min}}$) are shown for blood glucose levels. Data presented as $\text{mean} \pm \text{SEM}$ ($n=3-7$).

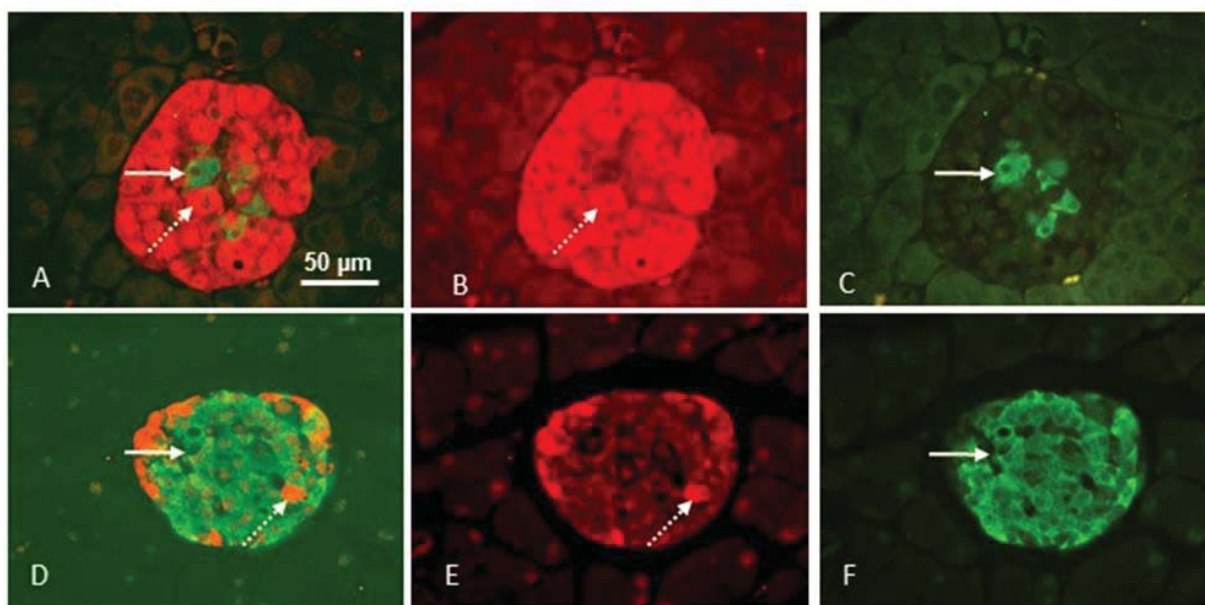
737

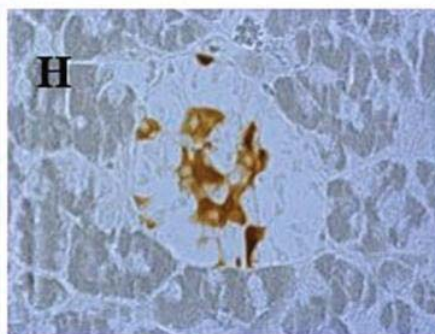
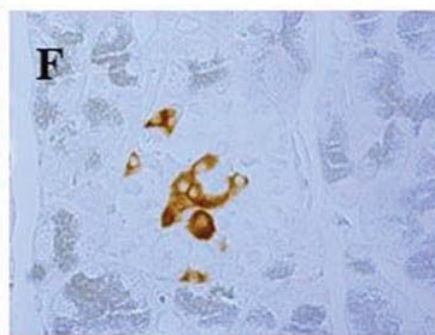
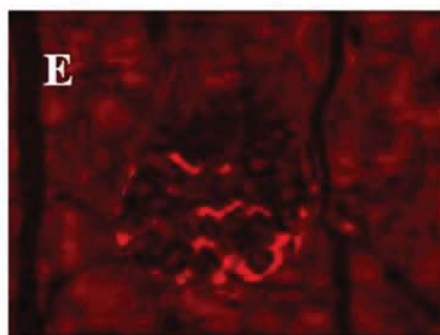
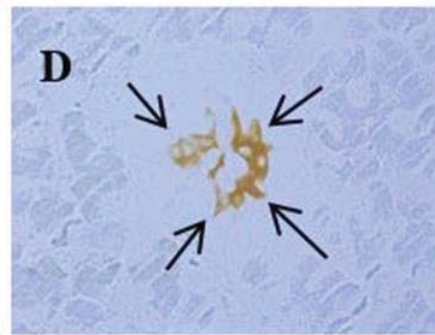
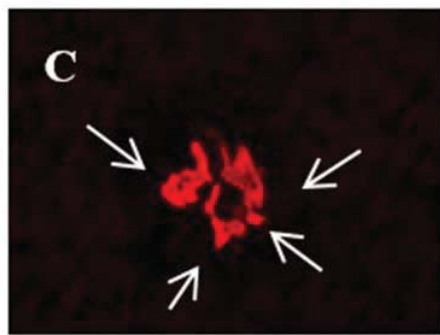
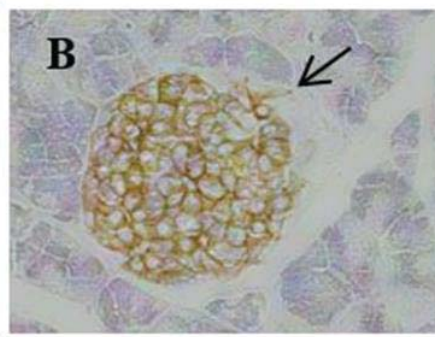
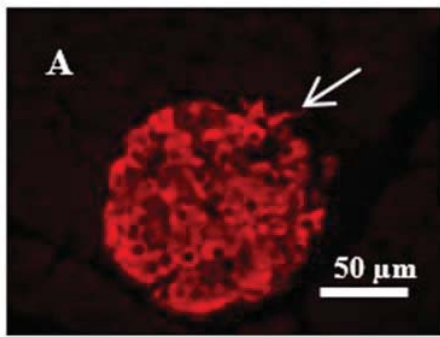
738
 739 **Table 1:** The components and concentrations of Vamin 14 Electrolytefree

<i>Amino acid</i>	<i>g/L</i>
Isoleucine	4.2
Leucine	5.9
Valine	5.5
Phenylalanine	5.9
Methionine	4.2
Lysine	6.8
Threonine	4.2
Tryptophan	1.4
Cysteine	0.42
Histidine	5.1
Tyrosine	0.17
Alanine	12.0
Arginine	8.4
Aspartic Acid	2.5
Glutamic Acid	4.2
Glycine	5.9
Proline	5.1
Serine	3.4

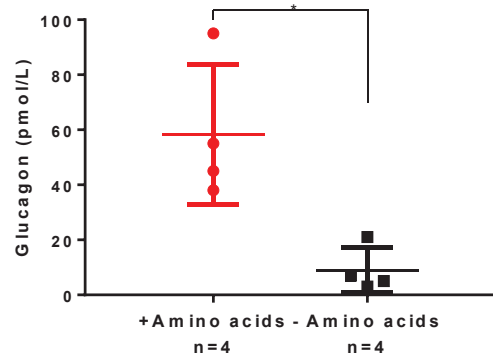








A



B

